Single Spin Asymmetries in charmonium production: NRQCD versus ICEM

A. V. Karpishkov[1,2], M. A. Nefedov[1], and V. A. Saleev[1,2]

[1] Samara National Research University
[2] Joint Institute for Nuclear Research

09.09.2020
SPD Physics and MC meeting

Outline

1. Generalized Parton Model (GPM) and it's application to calculation of SSA
   - Factorization formula for the GPM
   - Polarized production. SSA
2. Hadronization hypotheses: NRQCD and ICEM
   - NRQCD approach
   - ICEM approach
3. SSA in charmonium production at RHIC and NICA
   - Numerical results. Comparison to PHENIX data
   - Numerical results. Predictions for NICA
4. Conclusions

Generalized Parton Model (GPM) and it's application to calculation of SSA

Factorization schemes in different p_T-regions

The traditional Collinear Parton Model (CPM) is applicable in a region of high-p_T production

$$\mu \sim p_T \gg \Lambda_{QCD},$$

so we can neglect influence of small intrinsic $\mathbf{q_T}$ of initial partons ($\langle q_T^2 \rangle \simeq 1$ GeV^2).

But if we're interested in particle production in a region of $p_T \simeq \sqrt{\langle q_T^2 \rangle} \ll \mu$, we should take into account intrinsic q_T. It can be done within TMD approach, factorization for which has been proven in the limit $q_T \ll \mu$ [J. Collins, Camb. Monogr., Part. Phys. Nucl. Phys. Cosmol. 32, 1-624 (2011)]. In our case, the hard scale μ is given by charmonium mass $m_{\mathcal{C}} = 3.1 \div 3.7$ GeV.
So we can use phenomenological TMD-ansatz, a so called Generalized Parton Model (GPM), initial partons in which are on-shell:

$$q_\mu = xP_\mu^+ + yP_\mu^- + q_{T\mu}, (q_\mu)^2 = 0, \tag{1}$$

and a factorized prescription for TMD parton distribution functions (PDFs) is used:

$$F_a(x, q_T, \mu_F) = f_a(x, \mu_F) G_a(q_T), \tag{2}$$

where $f_a(x, \mu_F)$ – corresponding CPM PDF, $G_a(q_T)$ – Gaussian distribution $G_a(q_T) = \exp(-q_T^2 / \langle q_T^2 \rangle_a)/(\pi \langle q_T^2 \rangle_a)$.

Factorization formula for the GPM

Within the GPM we can write the following expression for the differential cross-section of $2 \to 1$ hard subprocess $g(q_1) + g(q_2) \to \mathcal{C}(k)$:

$$d\sigma(pp \to \mathcal{C}X) = \int dx_1 \int d^2\mathbf{q_{1T}} \int dx_2 \int d^2\mathbf{q_{2T}} \times \\ \times F_g(x_1, q_{1T}, \mu_F) F_g(x_2, q_{2T}, \mu_F) d\hat{\sigma}(gg \to \mathcal{C}), \quad (3)$$

where $\mathcal{C} = J/\psi, \psi(2S)$ or $\chi_c(1P)$, and

$$d\hat{\sigma}(gg \to \mathcal{C}) = (2\pi)^4 \delta^{(4)}(q_1 + q_2 - k) \frac{\overline{|M(gg \to \mathcal{C})|^2}}{2x_1 x_2 s} \frac{d^4k}{(2\pi)^3} \delta_+(k^2 - m_{\mathcal{C}}^2). \quad (4)$$

In a case of $2 \to 2$ subprocess $g(q_1) + g(q_2) \to \mathcal{C}(k) + g(q_3)$, $\mathcal{C} = J/\psi, \psi(2S)$ in formula (3) $d\hat{\sigma}(gg \to \mathcal{C})$ must be replaced by:

$$d\hat{\sigma}(gg \to \mathcal{C}g) = (2\pi)^4 \delta^{(4)}(q_1 + q_2 - k - q_3) \frac{\overline{|M(gg \to \mathcal{C}g)|^2}}{2x_1 x_2 s} \frac{d^3k}{(2\pi)^3 2k_0} \frac{d^4q_3}{(2\pi)^3} \delta_+(q_3^2). \quad (5)$$

Four-momenta of initial partons are on mass-shell ($q_1^2 = q_2^2 = 0$) and have longitudinal (along the Z-axis) and transverse parts:

$$q_1^\mu = \left(x_1 \frac{\sqrt{s}}{2} + \frac{\mathbf{q}_{1T}^2}{2\sqrt{s}x_1}, \mathbf{q}_{1T}, x_1 \frac{\sqrt{s}}{2} - \frac{\mathbf{q}_{1T}^2}{2\sqrt{s}x_1} \right)^\mu, \quad (6)$$

$$q_2^\mu = \left(x_2 \frac{\sqrt{s}}{2} + \frac{\mathbf{q}_{2T}^2}{2\sqrt{s}x_2}, \mathbf{q}_{2T}, -x_2 \frac{\sqrt{s}}{2} + \frac{\mathbf{q}_{2T}^2}{2\sqrt{s}x_2} \right)^\mu. \quad (7)$$

Single Spin Asymmetry

In inclusive process $p^{\uparrow}p \to \mathcal{C}X$ $\mathcal{C} = J/\psi, \chi_c, \psi(2S))$ SSA is defined as:

$$A_N = \frac{d\sigma^{\uparrow} - d\sigma^{\downarrow}}{d\sigma^{\uparrow} + d\sigma^{\downarrow}} = \frac{d\Delta\sigma}{2d\sigma}. \tag{8}$$

The numerator and denominator of A_N have the form:

$$d\sigma \propto \int dx_1 \int d^2q_{1T} \int dx_2 \int d^2q_{2T} F_g(x_1, q_{1T}, \mu_F) F_g(x_2, q_{2T}, \mu_F) d\hat{\sigma}(gg \to \mathcal{C}X), \tag{9}$$

$$d\Delta\sigma \propto \int dx_1 \int d^2q_{1T} \int dx_2 \int d^2q_{2T} \big[\hat{F}_g^{\uparrow}(x_1, \mathbf{q}_{1T}, \mu_F) - \hat{F}_g^{\downarrow}(x_1, \mathbf{q}_{1T}, \mu_F)\big] \times F_g(x_2, q_{2T}, \mu_F) d\hat{\sigma}(gg \to \mathcal{C}X), \tag{10}$$

where $\hat{F}_g^{\uparrow,\downarrow}(x, q_T, \mu_F)$ is the distribution of unpolarized gluon (or quark) in polarized proton.
Following the Trento conventions [A. Bacchetta, U. DAlesio, M. Diehl and C. A. Miller, Phys. Rev. D **70**, 117504 (2004)], the gluon Sivers function (GSF) can be introduced as

$$\begin{aligned} \Delta\hat{F}_g^{\uparrow}(x_1, \mathbf{q}_{1T}, \mu_F) &\equiv \hat{F}_g^{(\uparrow)}(x_1, \mathbf{q}_{1T}, \mu_F) - \hat{F}_g^{(\downarrow)}(x_1, \mathbf{q}_{1T}, \mu_F) \\ &= \Delta^N F_g^{\uparrow}(x_1, \mathbf{q}_{1T}^2, \mu_F) \cos(\phi_1). \end{aligned} \tag{11}$$

Moreover, GSF must satisfy the positivity bound $\forall\ x_1, q_{1T}$:

$$\left|\Delta^N F_g^{\uparrow}(x_1, \mathbf{q}_{1T}^2, \mu_F)\right| \leq 2F_g(x_1, q_{1T}, \mu_F). \tag{12}$$

Hadronization hypotheses: NRQCD and ICEM

Basics of NRQCD factorization

The NRQCD framework [G. T. Bodwin, E. Braaten, and G. P. Lepage, Phys. Rev. D **51**, 1125 (1995)] describes heavy quarkonia in terms of Fock state decompositions. In case of orthoquarkonium state the wave function can be written as power series expansion in the velocity parameter $v \sim 1/\ln M_Q$:

$$|\mathcal{H}\rangle = \mathcal{O}(v^0)|Q\bar{Q}[^3S_1^{(1)}]\rangle + \mathcal{O}(v)|Q\bar{Q}[^3P_J^{(8)}]g\rangle + \mathcal{O}(v^2)|Q\bar{Q}[^1S_0^{(8)}]g\rangle \quad (13)$$

$$+\mathcal{O}(v^2)|Q\bar{Q}[^3S_1^{(1,8)}]gg\rangle + \ldots \quad (14)$$

In the NRQCD effects of short and long distances are separated, and then the cross-section of heavy-quarkonium production via a partonic subprocess $a + b \to \mathcal{H} + X$ can be presented in a factorized form:

$$d\hat{\sigma}(a + b \to \mathcal{H} + X) = \sum_n d\hat{\sigma}(a + b \to Q\bar{Q}[n] + X) \times \langle \mathcal{O}^{\mathcal{H}}[n]\rangle, \quad (15)$$

where n denotes the set of quantum numbers of the $Q\bar{Q}$ pair, and its nonperturbative transitions into $\mathcal{H}$ is described by the NMEs $\langle \mathcal{O}^{\mathcal{H}}[n]\rangle$.
In the general case, the partonic cross-section of quarkonium production from the $Q\bar{Q}$ Fock state $n = {}^{2S+1}L_J^{(1,8)}$ has the form:

$$d\hat{\sigma}(a + b \to Q\bar{Q}[^{2S+1}L_J^{(1,8)}] \to \mathcal{H}) = d\hat{\sigma}(a + b \to Q\bar{Q}[^{2S+1}L_J^{(1,8)}]) \times \frac{\langle \mathcal{O}^{\mathcal{H}}[^{2S+1}L_J^{(1,8)}]\rangle}{N_{col}N_{pol}},$$

where $N_{col} = 2N_c$ for color-singlet state, $N_{col} = N_c^2 - 1$ for color-octet state, and $N_{pol} = 2J + 1$.

Amplitude of specified state

The definition of partonic cross-section of $Q\bar{Q}[^{2S+1}L_J^{(1,8)}]$ production is following:

$$d\hat{\sigma}(a+b\to Q\bar{Q}[^{2S+1}L_J^{(1,8)}]) = \frac{1}{2x_1x_2S}\overline{|\mathcal{A}(a+b\to Q\bar{Q}[^{2S+1}L_J^{(1,8)}])|^2}d\Phi. \quad (16)$$

The projectors on spin-zero and spin-one states:

$$\Pi_0 = \frac{1}{8m^3}\left(\frac{\hat{p}}{2}-\hat{q}-m\right)\gamma^5\left(\frac{\hat{p}}{2}+\hat{q}+m\right), \Pi_1^\alpha = \frac{1}{8m^3}\left(\frac{\hat{p}}{2}-\hat{q}-m\right)\gamma^\alpha\left(\frac{\hat{p}}{2}+\hat{q}+m\right).$$

The projectors on color-singlet and color-octet states:

$$C_1 = \frac{\delta_{ij}}{\sqrt{N_c}},\ C_8 = \sqrt{2}T^a_{ij},$$

respectively, where T^a with $a = 1,\cdots,N_c^2-1$ are the generators of the color gauge group $SU(N_c)$.
For example, the amplitude of $Q\bar{Q}$ production in state $^3S_1^{(1,8)}$ is:

$$\mathcal{A}(a+b\to Q\bar{Q}[^3S_1^{(1,8)}]) = Tr[C_{1,8}\Pi_1^\alpha\times\mathcal{A}(a+b\to Q\bar{Q})\varepsilon_\alpha(p)]_{q=0},$$

where $\varepsilon_\alpha(p)$ is the polarization 4-vector of a spin-one particle with momentum p^μ and mass $M=p^2$. And the polarization sum then is:

$$\sum_{J_z}\varepsilon_\alpha(p)\varepsilon^*_{\alpha'}(p) = \mathcal{P}_{\alpha\alpha'}(p) = -g_{\alpha\alpha'}+\frac{p_\alpha p'_\alpha}{M^2}.$$

Long- and short-distance matrix elements

We adopt the following values of color-singlet LDMEs [R. Barbieri, M. Caffo, R. Gatto and E. Remiddi (1981)]: $\langle \mathcal{O}^{J/\psi}[^3S_1^{(1)}]\rangle = 1.3$ GeV^3, $\langle \mathcal{O}^{\psi'}[^3S_1^{(1)}]\rangle = 6.5 \times 10^{-1}$ GeV^3 and $\langle \mathcal{O}^{\chi_{cJ}}[^3P_J^{(1)}]\rangle = (2J+1) \times 8.9 \times 10^{-2}$ GeV^5. Squared LO in α_S amplitudes for $2 \to 1$ subprocesses in CPM are well-known [P.L. Cho, A.K. Leibovich (1996)]:

$$\overline{|\mathcal{A}(g+g \to \mathcal{C}[^3P_0^{(1)}]|^2} = \frac{8}{3}\pi^2\alpha_s^2 \frac{\langle \mathcal{O}^{\mathcal{C}}[^3P_0^{(1)}]\rangle}{M^3}, \quad (17)$$

$$\overline{|\mathcal{A}(g+g \to \mathcal{C}[^3P_1^{(1)}]|^2} = 0, \quad (18)$$

$$\overline{|\mathcal{A}(g+g \to \mathcal{C}[^3P_2^{(1)}]|^2} = \frac{32}{45}\pi^2\alpha_s^2 \frac{\langle \mathcal{O}^{\mathcal{C}}[^3P_2^{(1)}]\rangle}{M^3}, \quad (19)$$

$$\overline{|\mathcal{A}(g+g \to \mathcal{C}[^3S_1^{(8)}]|^2} = 0, \quad (20)$$

$$\overline{|\mathcal{A}(g+g \to \mathcal{C}[^1S_0^{(8)}]|^2} = \frac{5}{12}\pi^2\alpha_s^2 \frac{\langle \mathcal{O}^{\mathcal{C}}[^1S_0^{(8)}]\rangle}{M}, \quad (21)$$

$$\overline{|\mathcal{A}(g+g \to \mathcal{C}[^3P_0^{(8)}]|^2} = 5\pi^2\alpha_s^2 \frac{\langle \mathcal{O}^{\mathcal{C}}[^3P_0^{(8)}]\rangle}{M^3}, \quad (22)$$

$$\overline{|\mathcal{A}(g+g \to \mathcal{C}[^3P_1^{(8)}]|^2} = 0, \quad (23)$$

$$\overline{|\mathcal{A}(g+g \to \mathcal{C}[^3P_2^{(8)}]|^2} = \frac{4}{3}\pi^2\alpha_s^2 \frac{\langle \mathcal{O}^{\mathcal{C}}[^3P_2^{(8)}]\rangle}{M^3}, \quad (24)$$

Long- and short-distance matrix elements

There is only one relevant LO in α_S $2 \to 2$ partonic subprocess, which describes direct production of J/ψ or $\psi(2S)$ via color-singlet intermediate state $[^3S_1^{(1)}]$ as it is in the Color-Singlet Model.
The squared amplitude for this partonic subprocess reads [R. Gastmans, W. Troost and T. T. Wu, Phys. Lett. B **184**, 257-260 (1987)]:

$$\overline{|\mathcal{A}(g+g \to \mathcal{C}[^3S_1^{(1)}]+g|^2} = \pi^3 \alpha_s^3 \frac{\langle \mathcal{O}^{\mathcal{C}}[^3S_1^{(1)}]\rangle}{M^3} \frac{320M^4}{81(M^2-\hat{t})^2(M^2-\hat{u})^2(\hat{t}+\hat{u})^2} \times$$
$$\times (M^4\hat{t}^2 - 2M^2\hat{t}^3 + \hat{t}^4 + M^4\hat{t}\hat{u} - 3M^2\hat{t}^2\hat{u} + 2\hat{t}^3\hat{u} + M^4\hat{u}^2 -$$
$$- 3M^2\hat{t}\hat{u}^2 + 3\hat{t}^2\hat{u}^2 - 2M^2\hat{u}^3 + 2\hat{t}\hat{u}^3 + \hat{u}^4). \quad (25)$$

Improved Color Evaporation Model (ICEM)

In the CEM, it is assumed that all $c\bar{c}$ pairs with invariant masses below the $D\bar{D}$-threshold hadronize to charmonia with some probability, which is independent from angular momentum and spin quantum numbers of the pair:

$$\frac{d\sigma^{\mathcal{C}}}{d^3k} = F_{\mathcal{C}} \times \int_{4m_c^2}^{4m_D^2} dM_{c\bar{c}}^2 \frac{d\sigma^{c\bar{c}}}{dM_{c\bar{c}}^2 d^3k}, \tag{26}$$

where $F_{\mathcal{C}}$ is the process-independent hadronization probability to the charmonium state $\mathcal{C}$. Within the framework of the traditional CEM [H. Fritzsch, Phys. Lett. B **67**, 217 (1977); F. Halzen, Phys. Lett. B **69**, 105 (1977)] differential distributions of different quarkonium states are assumed to be identical. The ratios between the distributions of any two charmonium family members are independent of their kinematics. That disadvantage has been corrected recently [Y.Q. Ma and R. Vogt, Phys. Rev. D **94** (2016) 114029].
ICEM sets a larger limit on $M_{c\bar{c}}$ as $M_{\mathcal{C}}$ than $2m_c$, that is significantly different from the traditional CEM. Thus, follow the formulation of ICEM in the work [V. Cheung and R. Vogt, Phys. Rev. D **98** (2018) 114029]:

$$\frac{d\sigma^{\mathcal{C}}}{d^3k} = F_{\mathcal{C}} \times \int_{M_{\mathcal{C}}^2}^{4m_D^2} dM_{c\bar{c}}^2 \frac{d\sigma^{c\bar{c}}}{dM_{c\bar{c}}^2 d^3k}. \tag{27}$$

Cross section of the ICEM

That is leading us to the following result in GPM:

$$\begin{aligned}\frac{d\sigma^{\mathcal{C}}}{d^3k} &= F_{\mathcal{C}} \times \int dx_1 \int d^2q_{1T} \int dx_2 \; F_g(x_1, q_{1T}, \mu_F) F_g(x_2, q_{2T}, \mu_F) \hat{\sigma}(\hat{s}, ij \to c\bar{c}) \\ &\times \delta(q_1^3 + q_2^3 - k^3) \left[\theta(\hat{s} - m_{\mathcal{C}}^2) - \theta(\hat{s} - 4m_D^2)\right], \end{aligned} \tag{28}$$

where $\hat{\sigma}(\hat{s}, ij \to c\bar{c})$ is just a well-known total cross section of one of the subprocesses: $gg \to c\bar{c}$ or $q\bar{q} \to c\bar{c}$, correspondingly.

SSA in charmonium production at RHIC and NICA

PHENIX-2012 data, $|y| \leq 0.35$, $\sqrt{S} = 200$ GeV.

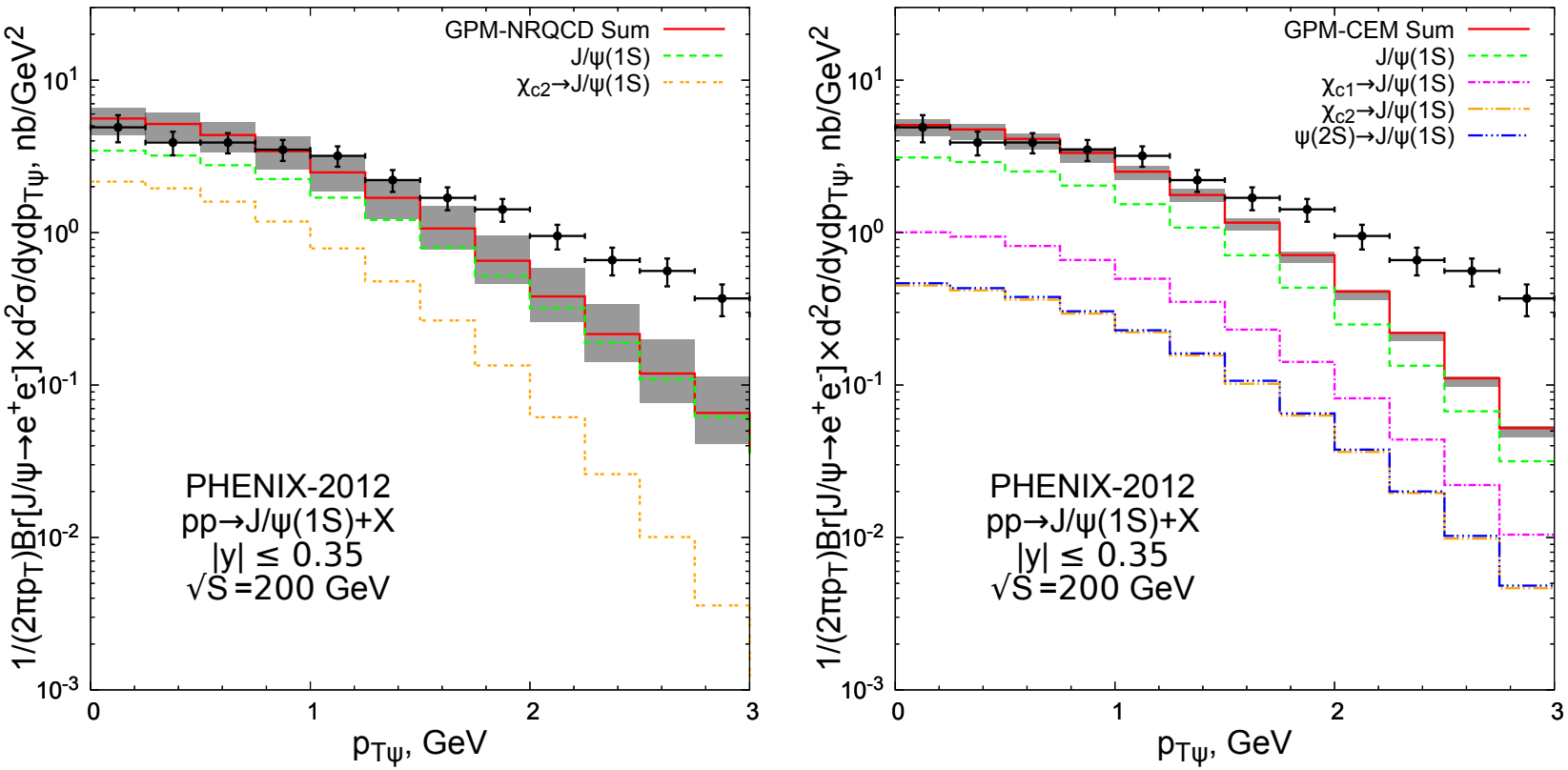

Figure 1 : Differential cross-section of prompt J/ψ production as function of transverse momentum at $\sqrt{s} = 200$ GeV, $|y| \leq 0.35$. The theoretical results are obtained in GPM with $\langle q_T^2 \rangle = 1$ GeV^2. Left panel: NRQCD-factorization prediction with only color-singlet channels included. Right panel: ICEM-prediction. In the left panel, non-zero contributions from decays $\chi_{c0,1} \to J/\psi$ and $\psi(2S) \to J/\psi$ are not shown. Experimental data are from the Ref. [A. Adare *et al.* [PHENIX], Phys. Rev. D **85**, 092004 (2012)].

PHENIX-2012 data, $|y| \leq 0.35$, $\sqrt{S} = 200$ GeV.

Table 1 : The relative contributions of direct and feed-down production within NRQCD and ICEM. Experimetal data of the PHENIX collaboration for $\sqrt{s} = 200$ GeV are from [A. Adare *et al.* [PHENIX], Phys. Rev. D **85**, 092004 (2012)].

$\sqrt{s}$	Model/Source of data	$\sigma^{\text{direct}} : \sigma^{\chi_c \to J/\psi} : \sigma^{\psi(2S) \to J/\psi}$
24 GeV	NRQCD	0.58 : 0.39 : 0.03
	ICEM	0.68 : 0.25 : 0.07
200 GeV	NRQCD	0.61 : 0.34 : 0.05
	ICEM	0.61 : 0.30 : 0.09
200 GeV	PHENIX collab.	0.58 : 0.32 : 0.10

Table 2 : The values of hadronization probabilities of ICEM, which had been obtained via the fit of total cross-section of J/ψ-production at PHENIX. The fit of LHC data are taken from [V. Cheung and R. Vogt, Phys. Rev. D **98**, 114029 (2018)].

$F_{\mathcal{C}}$	Our fit	The fit of LHC data
$F_{J/\psi}$	0.02	0.02
$F_{\chi c1}$	0.06	0.18
$F_{\chi c2}$	0.06	0.2
$F_{\psi'}$	0.08	0.12

PHENIX-2018 data, $1.2 \leq |y| \leq 2.2$, $\sqrt{S} = 200$ GeV.

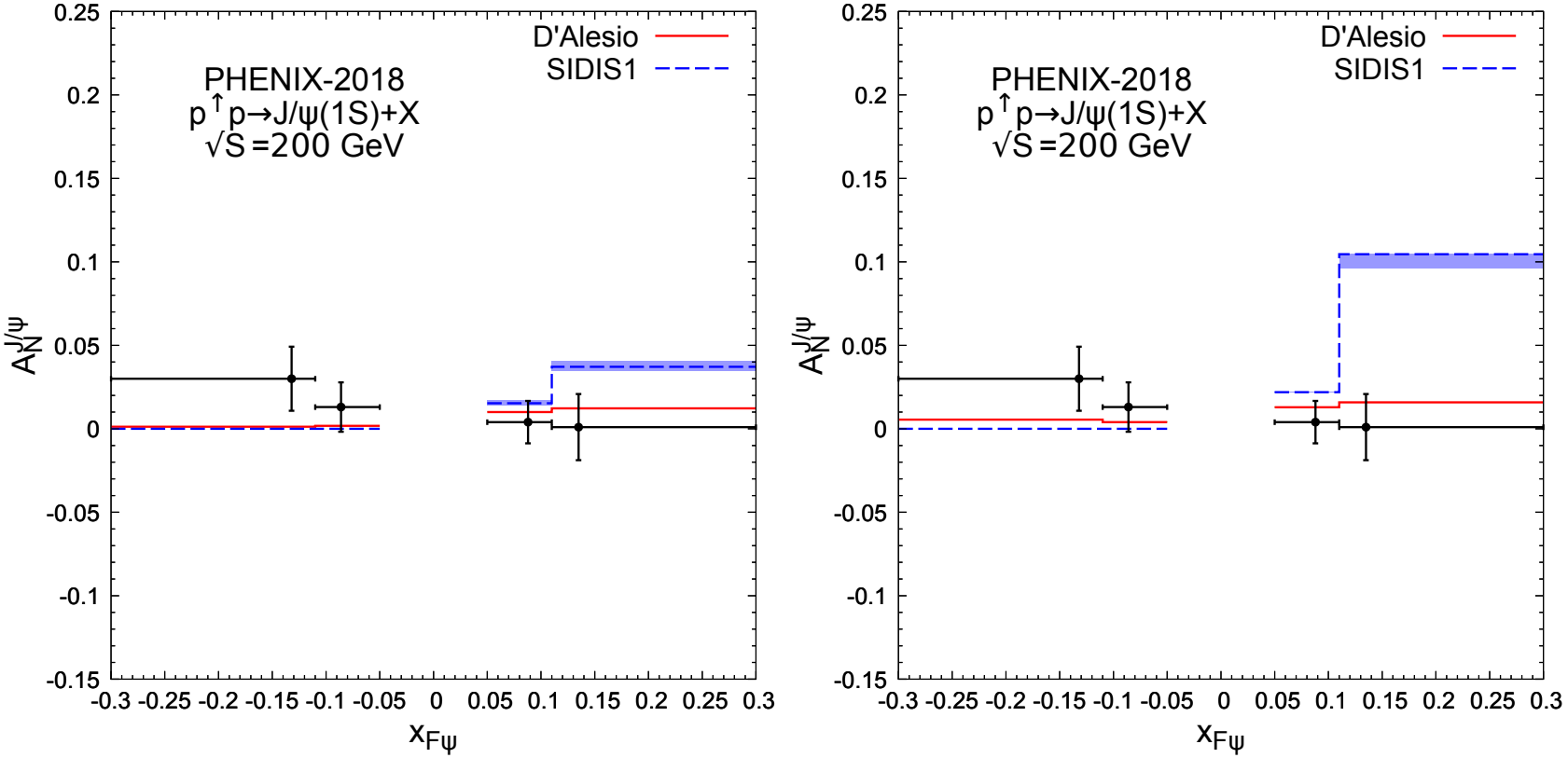

Figure 2 : SSA $A_N^{J/\psi}$ as function of x_F at $\sqrt{s} = 200$ GeV. The theoretical results are obtained with SIDIS1 and D'Alesio *et al.* parameterizations of GSFs. Experimental data are from Ref. [C. Aidala *et al.* [PHENIX], Phys. Rev. D **98**, 012006 (2018)]. Left panel: NRQCD-prediction. Right panel: ICEM prediction.

PHENIX-2018 data, $1.2 \leq |y| \leq 2.2$, $\sqrt{S} = 200$ GeV.

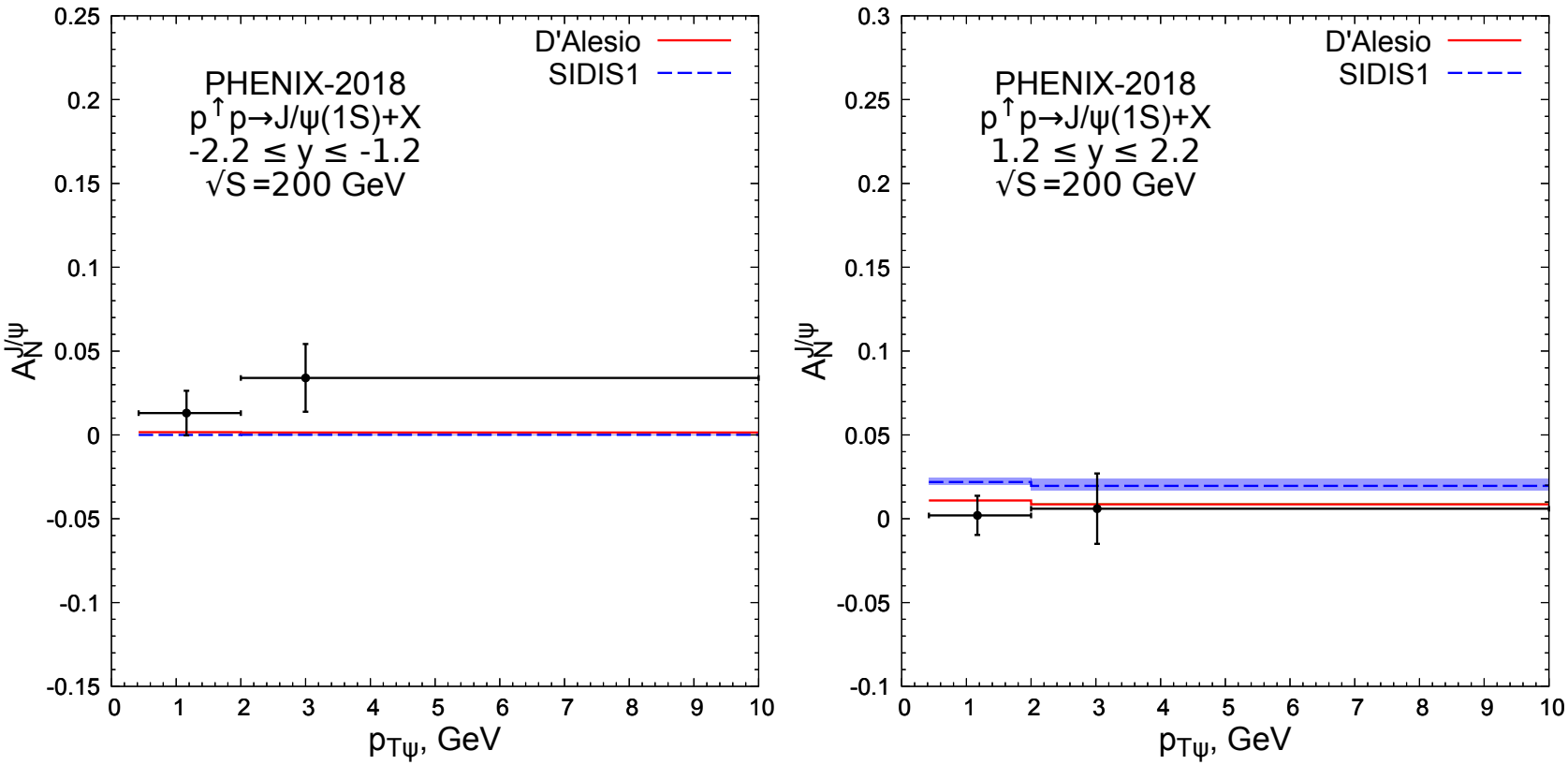

Figure 3 : NRQCD predictions for SSA $A_N^{J/\psi}$ as function of J/ψ-transverse momentum at $\sqrt{s} = 200$ GeV. The theoretical results are obtained with SIDIS1 and D'Alesio et al. parameterizations of GSFs. Left panel – backward production ($-2.2 \leq y \leq -1.2$), right panel – forward production ($1.2 \leq y \leq 2.2$). Experimental data are from Ref. [C. Aidala *et al.* [PHENIX], Phys. Rev. D **98**, 012006 (2018)].

PHENIX-2018 data, $1.2 \leq |y| \leq 2.2$, $\sqrt{S} = 200$ GeV.

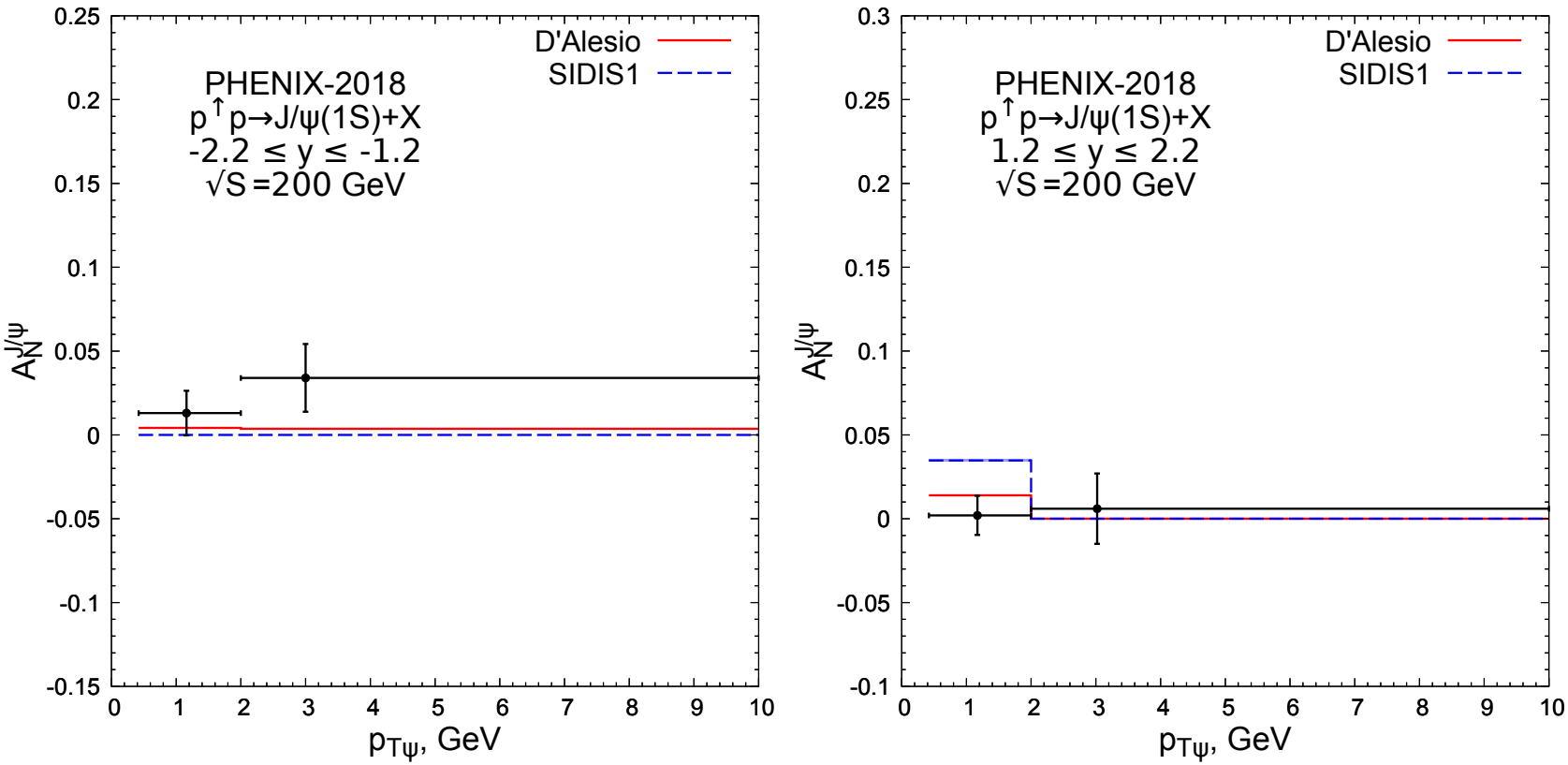

Figure 4 : ICEM predictions for SSA $A_N^{J/\psi}$ as function of J/ψ-transverse momentum at $\sqrt{s} = 200$ GeV. The theoretical results are obtained with SIDIS1 and D'Alesio et al. parameterizations of GSFs. Left panel – backward production ($-2.2 \leq y \leq -1.2$), right panel – forward production ($1.2 \leq y \leq 2.2$). Experimental data are from Ref. [C. Aidala *et al.* [PHENIX], Phys. Rev. D **98**, 012006 (2018)].

Predictions for NICA (in different models), $|y| \leq 3$, $\sqrt{S} = 24$ GeV.

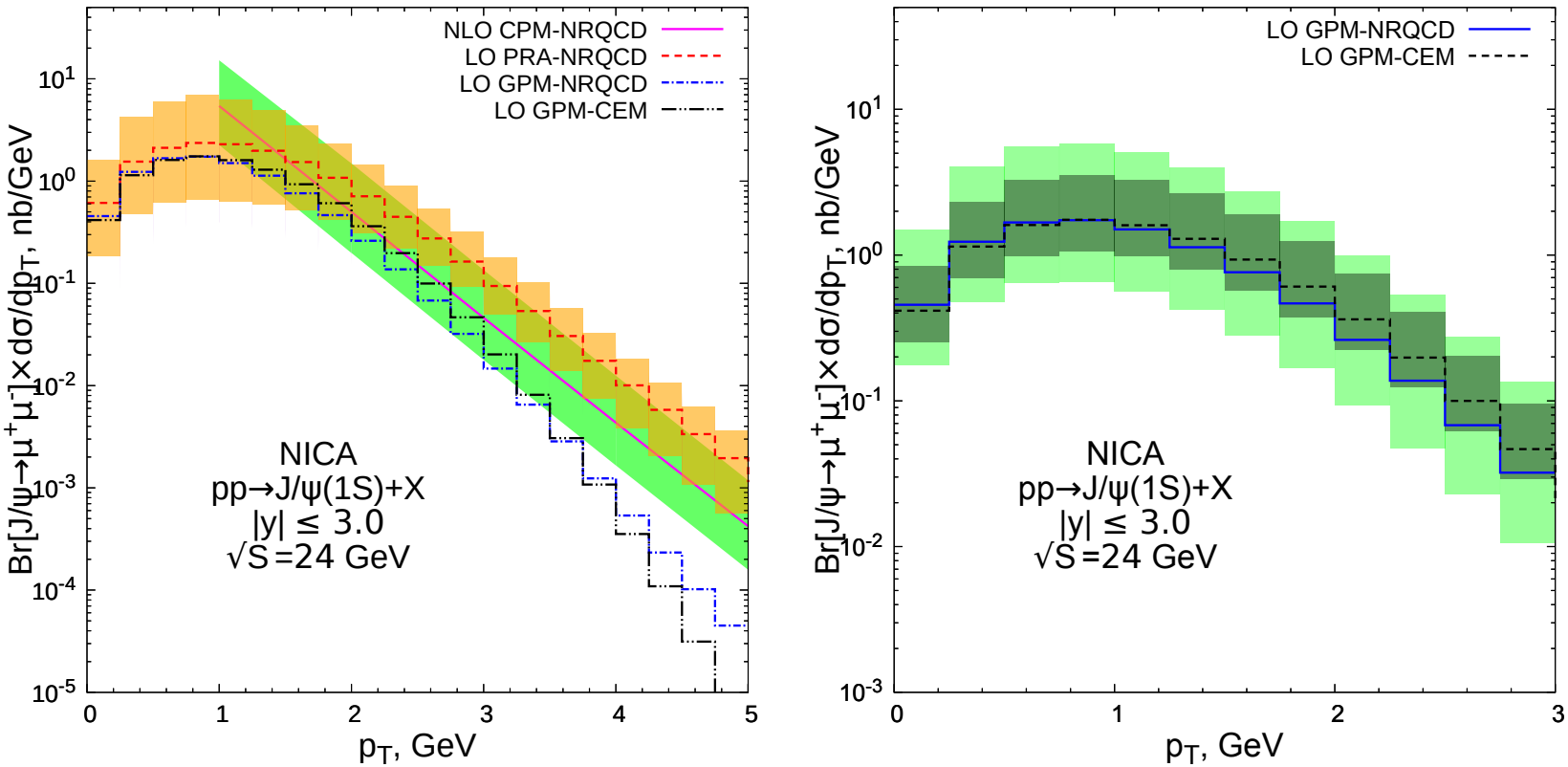

Figure 5 : Prompt J/ψ transverse momentum distribution at $\sqrt{s} = 24$ GeV, $|y| \leq 3$. Left panel: GPM results with $\langle q_T^2 \rangle = 1$ GeV^2 are shown by dash-dotted (NRQCD) and dash-double-dotted (ICEM) histograms. Solid and dashed histograms with uncertainty bands are PRA [A.V. Karpishkov, M.A. Nefedov and V.A. Saleev, J. Phys. Conf. Ser. **1435**, 012015 (2020)] and NLO CPM [M. Butenschön and B.A. Kniehl, private communication] predictions respectively. Right panel: GPM predictions in NRQCD (solid histogram with light green uncertainty band) and ICEM (dashed histogram with dark-green uncertainty band) approaches with their uncertainty bands shown.

Predictions for SSA at NICA (SIDIS1), $|y| \leq 3$, $\sqrt{S} = 24$ GeV.

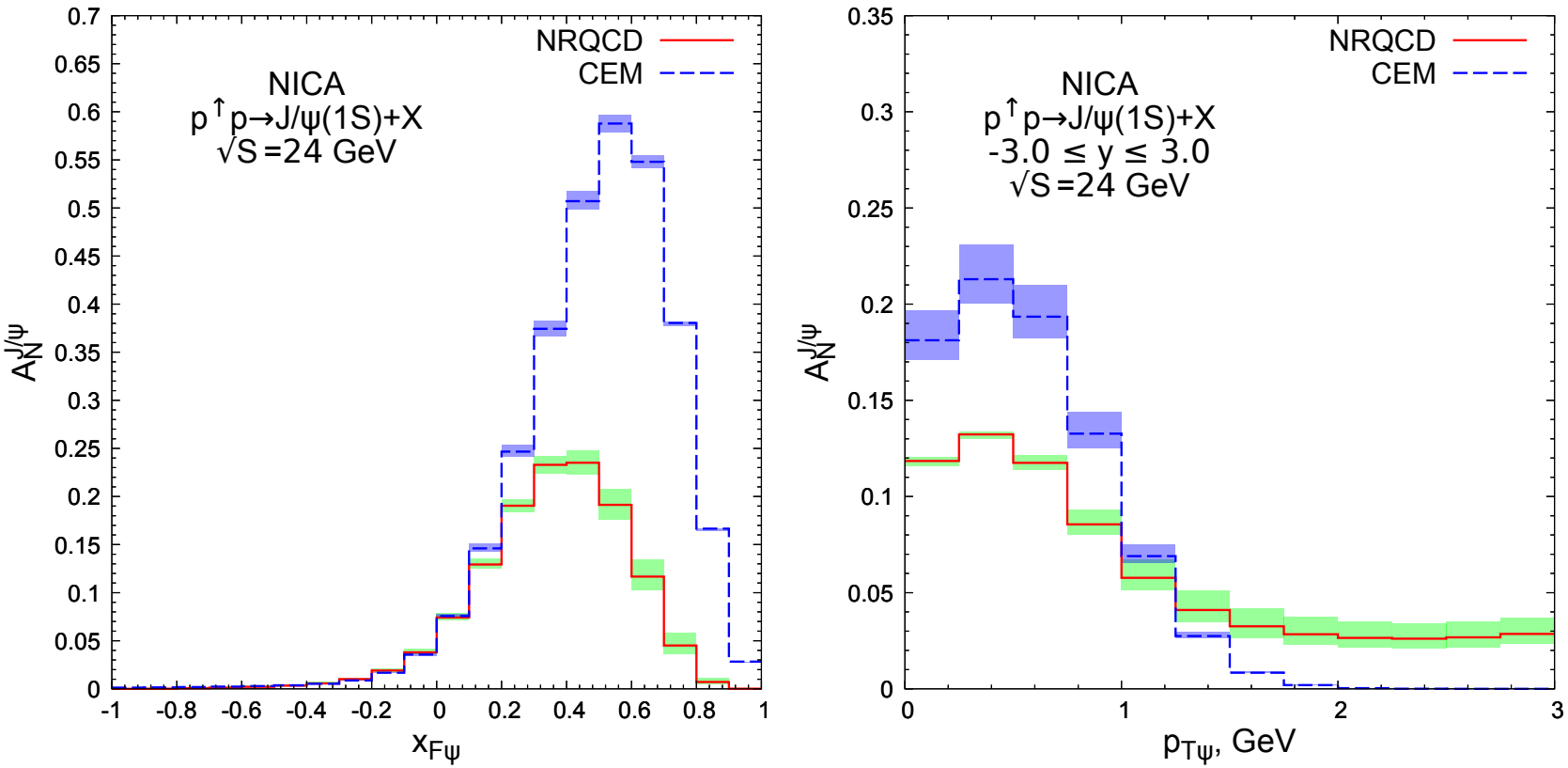

Figure 6 : Comparison of predictions for SSA $A_N^{J/\psi}$ as function of x_F (left panel) and transverse momentum (right panel) at $\sqrt{s} = 24$ GeV in NRQCD (solid histogram) and ICEM (dashed histogram) approaches. The SIDIS1 parametrisation of GSFs is used.

Predictions for SSA at NICA (D'Alesio), $|y| \leq 3$, $\sqrt{S} = 24$ GeV.

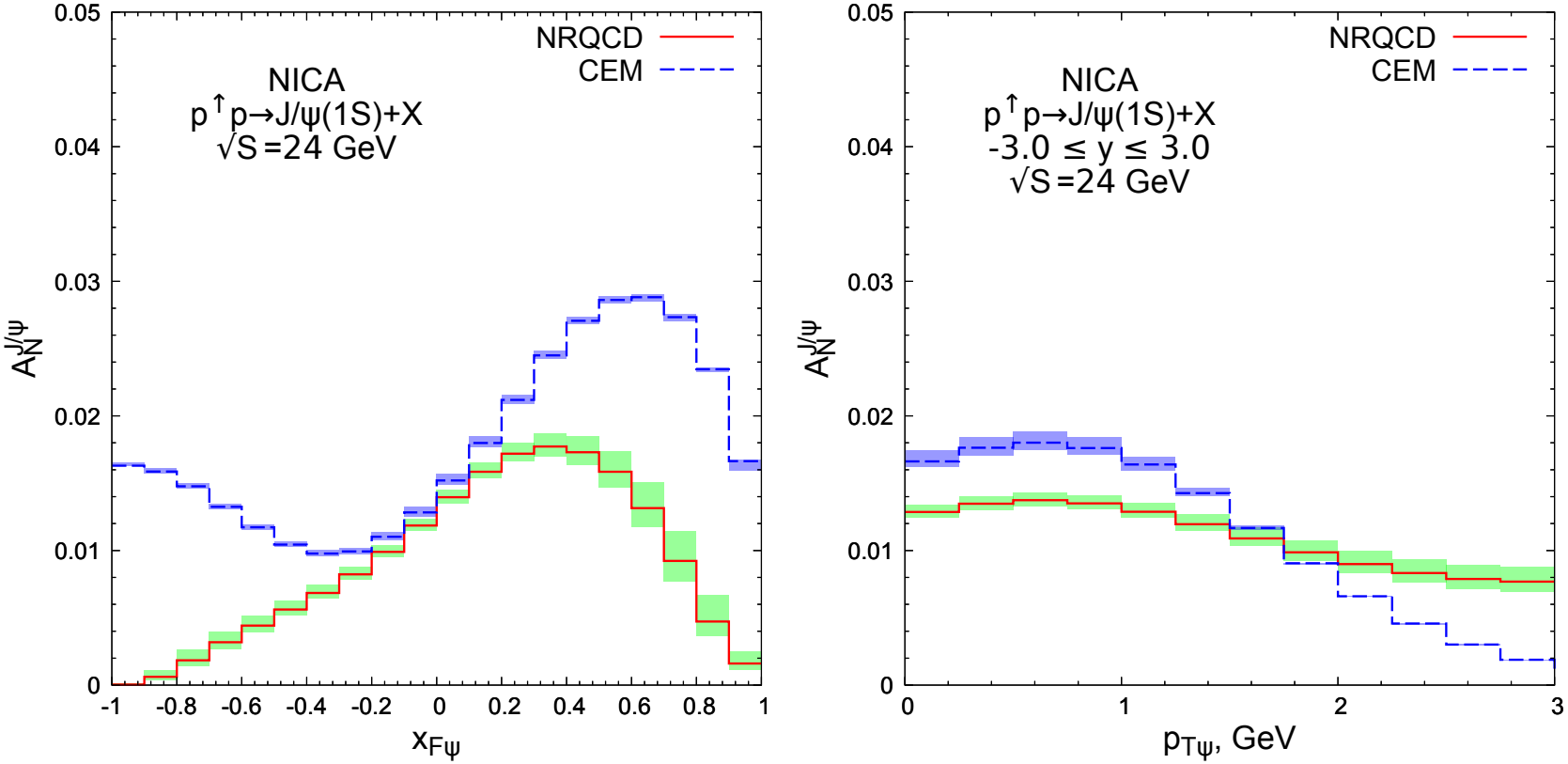

Figure 7 : Comparison of predictions for SSA $A_N^{J/\psi}$ as function of x_F (left panel) and transverse momentum (right panel) at $\sqrt{s} = 24$ GeV in NRQCD (solid histogram) and ICEM (dashed histogram) approaches. The D'Alesio *et al.* parametrisation of GSFs is used.

Conclusions

- We have found that taking into account only color-singlet production mechanism, the good description of prompt J/ψ transverse momentum spectra at small $k_{T\,J/\psi} < m_{J/\psi}$ can be achieved in GPM. Our NRQCD calculation leads to total cross-section ratios of direct and feed-down contributions in good agreement with experimental data.
- We find, that SIDIS1 parametrisation for gluon Sivers function contradicts PHENIX data, while parametrisation of D'Alesio *et al.* leads to reasonable predictions for magnitude, J/ψ transverse momentum and $x_{F\psi}$ dependence of the asymmetry.
- We demonstrate measurable differences in predictions of transverse SSAs obtained in NRQCD versus ICEM, especially at SPD NICA experiment.
- We conclude that we can safely perform predictions for SSA at NICA energies.

Our results you can find as an arXiv preprint [A.V. Karpishkov, M.A. Nefedov, V.A. Saleev, arXiv:2008.07232].

Thank you for your attention!